Effect of *Grewia* spp. biopolymer on floc properties of coagulated laterite suspension

Kameni Ngounou M. Bernard[a,b], Prakash V. Bobde[a], Ndi K. Sylvere[b], Kofa G. Patrice[b], Kayem G. Joseph[b], Sukdeb Pal[a,c,]*

[a]*Wastewater Technology Division (WWTD), Council of Scientific and Industrial Research-National Environmental Engineering Research Institute (CSIR-NEERI), Nagpur - 440020, India, Tel. +91-712-2249885 Ext. 693; email: s_pal@neeri.res.in (S. Pal), Tel. +237-699433882; emails: kameningounoumichelbernard@gmail.com (K.N.M. Bernard), bobdeprakash5@gmail.com (P.V. Bobde)*
[b]*Industrial Filtration and Water Treatment (Chem. Eng.) Group, Department of Process Engineering, ENSAI, University of Ngaoundere, Cameroon, Tel. +237-699705655; email: ndikoungou@yahoo.fr (N.K. Sylvere), Tel. +237-695665984; email: guikofa@yahoo.fr (K.G. Patrice), Tel. +237-677644872; email: gjkayem@yahoo.fr (K.G. Joseph)*
[c]*Academy of Scientifc and Innovative Research (AcSIR), Ghaziabad - 201002, India*

ABSTRACT

Effect of *Grewia* spp. biopolymer on the morphological characteristics and strength of laterite flocs coagulated using two common inorganic coagulants was studied. Physicochemical properties of the biopolymer obtained from *Grewia* spp. barks were determined using elemental analysis, gel permeation chromatography, zeta potential measurement, IR and NMR spectroscopy, etc. Zeta potential (-24.64 ± 0.49 mV) measured in aqueous medium at pH 7 revealed that the polymer is anionic in nature. Polysaccharides were identified as the major constituent of the polymer responsible for its flocculation property. Aqueous laterite suspension was subjected to jar test at different pH using iron $[Fe_2(SO_4)_3]$ or alum $[Al_2(SO_4)_3]$ as coagulant either alone or in combination with *Grewia* spp. biopolymer. The fractal characteristics of the flocs under different experimental conditions were investigated using a non-invasive image analysis tool. Floc properties were found to be dependent on the pH of the aqueous suspension. Compact flocs were formed in lower pH. An increase in pH resulted in a looser floc structure. *Grewia* spp. biopolymer in combination with iron or alum resulted in more compact floc formation. Fractal dimensions of only iron-coagulated flocs having floc strength 51.22%–59.94% increased from (1.27 ± 0.09, 1.29 ± 0.06 and 1.23 ± 0.04) to (1.84 ± 0.12, 1.75 ± 0.14 and 1.62 ± 0.09) at pH 5, 7 and 9, respectively with floc strength as high as 81.58%–94.99%. Only alum-coagulated flocs having floc strength ranging between 54.81% and 56.38% and fractal dimensions 1.24 ± 0.06, 1.28 ± 0.07 and 1.23 ± 0.07 at pH 5, 7 and 9, respectively became more compact in presence of the biopolymer (floc strength 87.30%–91.80% and fractal dimensions 1.75 ± 0.07, 1.64 ± 0.08, 1.62 ± 0.11 at pH 5, 7 and 9, respectively). The present study demonstrates that *Grewia* spp. biopolymer has the potential to be used as an effective coagulant aid over a wide pH range.

Keywords: Laterite; *Grewia* spp. biopolymer; Fractal dimension; Floc structure; Floc strength

* Corresponding author.

1. Introduction

Coagulation–flocculation is one of the widely used processes that have found applications both in potable as well as wastewater treatment due to its simplicity and efficiency in solid–liquid separation [1,2]. There are many operational parameters including, pH, the density difference between the solid particles and liquid as well as physicochemical characteristics of coagulants and flocculant polymers that dictate the efficacy of this process [3] and determine the properties of flocs generated. Understanding of floc properties is of particular significance for optimizing the efficiency of the solid/liquid separation process. Previous studies reported that the structures of flocs could be explained using fractal dimension theory [4]. The fractal dimension concept provides a viable option to describe floc properties and behavior. It is reported that the polymer conditioning of alum sludge led to an increase in floc size and floc density [5]. Flocculation using cationic tapioca starch was found to increase floc density [6]. Investigations on kaolin floc formed using different coagulants such as alum and polyaluminum chloride revealed partial reversibility of flocs post-breakage and regrowth process [7]. To a considerable extent, the regrowth of broken flocs indicated practically the full reversibility of floc formation using cationic polyelectrolytes [8]. It was specified that using aluminum sulfate coagulant complete recovery of kaolin flocs did not take place after breakage [9]. Regrown flocs got converted into smaller particles after repetitive formation, breakage, and regrowth several times [10]. In the majority of studies formation of kaolin, flocs were investigated using different hydrolyzing salts. However, kaolin clay is relatively less complex than laterite soil is rich in mineral deposits such as aluminum, nickel, cobalt, manganese and iron-based minerals found in tropical regions. Surface water treatment for potable use as well as mineral processing operations (after mining) in these regions generates a huge quantity of laterite muds rich in heavy metals in the form of oxy-hydroxides of these metals. However, to the best of our knowledge, until now there is no straightforward research on the characterization of laterite flocs under different coagulation mechanisms. Reduction in the number of inorganic coagulants and sludge volume is another challenge. The concentration demand for inorganic coagulants and the amount of sludge generated can be reduced by using synthetic polymer flocculants of high efficiency [11]. However, synthetic polymers are often non-biodegradable and certain of their residual monomers are carcinogenic in nature [12]. With the rising demand for environmentally friendly processes and materials, bio-flocculants, mainly owing to their biodegradability [13], have attracted a great deal of attention from the scientific community. Bio-flocculants possess negative charges and are observed to be less efficient when the suspended particulates are also negatively charged. Therefore, in order to extend the application of bio-flocculants in water treatment, synergetic action between conventional inorganic coagulants and bio-flocculants is being explored. Thus, the main objective of the present study was to explore the application of *Grewia* spp. biopolymer (GP) in combination with two common coagulants, alum (aluminum sulfate) and iron (ferric sulfate), in treatment of aqueous suspension of laterite clay, and to investigate the effect of the *Grewia* spp. GP on morphological properties and strength of laterite flocs a non-invasive imaging tool. The micrographs and fractal dimensions of laterite flocs formed in the presence of GP were compared with that of controls obtained using only inorganic coagulants.

2. Background theories

2.1. Fractal dimension

The self-similar structure of aggregates of colloidal particles formed in coagulation-flocculation is very often best described using fractal geometry [4]. The fractal theory offers a quantitative estimate of the space-filling capacity of aggregated particles with the practical information that the effective density of aggregates, recognized as fractal objects, decreases as their size increases. If an aggregated mass has a fractal arrangement, the relationship between the coagulated mass (M) and linear measure of its size (R) can be expressed as:

$$M(R) \propto R^{(D_F)} \tag{1}$$

where D_F is the mass fractal dimension [14]. The higher the D_F values, the more compact is the aggregate structure. Lower D_F values are associated with the formation of more open floc structures [15–17]. 'Size' R is usually considered as the radius of gyration of the aggregate. Nonetheless, the form of Eq. (1) is independent of the precise definition of R, and the largest diameter of an irregular aggregate may conveniently be taken as the measure of its size. Applicability of Eq. (1) over a wide range of aggregate sizes implies the self-similar structure of the aggregates that do not depend on the scale of observation or the degree of magnification.

2.2. Floc strength

Floc strength is of great importance in solid–liquid separation following orthokinetic flocculation. The floc strength factor relies on both the number and strength of inter-particle bonds [1]. Thus, denser or compact floc structures having more inter-particle contacts imply stronger flocs. Depending on the applied shear rate flocs can only grow to a certain limiting size (diameter) related to mass and D_F as shown above (Eq. (1)). When the stress on the floc surface is greater than the bonding within the particles, larger flocs tend to break down into smaller fragments which in turn can undergo further aggregation. The floc strength can be obtained by numerous factors [18,19]. In this study, the diameter of a formed floc (d_1) and the diameter of a broken floc (d_2) were used to compute the floc strength factor (S_F).

$$S_F = \frac{d_2}{d_1} \times 100\% \tag{2}$$

It is worth mentioning that large, low-density flocs can be formed in the presence of polymeric flocculants (interparticle-bonds are strong). Similarly, due to their lower size, smaller aggregates with weaker bonding can also have

a higher density. Polymeric flocculants facilitate the formation of more open but stronger flocs that can further increase in size under given shear conditions. Larger flocs having fractal character results in a lower density.

3. Materials and methods

3.1. Preparation of Grewia spp. biopolymer

Matured *Grewia* barks were collected from the north region of Cameroon. Photograph of *Grewia* spp barks is shown in Fig. 1. Crude GP was extracted following a previously reported method [20]. Briefly, the dried and pulverized *Grewia* spp. the bark was dispersed in water (1:80 w/v, pH 4) at 50°C for 4 h. The fibrous material from the dispersed mucilage was separated by straining through low temperature (4°C) centrifugation at 5300 rpm for 20 min. The crude polymer was precipitated using 3 volumes of 95% absolute ethanol and freeze-dried.

3.2. Laterite clay suspension

The laterite suspension used in this work was obtained by dispersing laterite clay (10 g/L) into 1 L of Milli Q water. The dispersion was then thoroughly mixed using a magnetic stirrer at 100 rpm for 6 h. Subsequently, the dispersion was allowed to settle for 24 h. The stable supernatant dispersion was used as stock laterite clay suspension.

3.3. Jar test

Jar test experiments were carried out at ambient temperature (25°C). Aluminum sulfate (Alum) and ferric sulfate (Iron) were used as coagulants. GP was used as a coagulant aid. Immediately after the addition of coagulant/coagulant aid, the suspension was flash mixed for an initial period of 5 min at 150 rpm, followed by slow mixing at 30 rpm for 15 min. Thereafter, the flocs were allowed to settle for 20 min. The pH of the laterite clay suspension was monitored and maintained at desired pH values (5, 7 and 9) adding acid (0.1 M HCl) or base (0.1 M NaOH) as required.

Fig. 1. Barks of *Grewia* spp.

3.4. Characterization of GP

The elemental analysis (C, H, N, and S) of the GP sample was performed using an elemental analyzer system (Vario MICRO cube, Germany) equipped with a TCD detector. The infrared spectrum was recorded using a Fourier-transform infrared (FTIR) spectrometer (Vertex 70, Bruker, Germany). The molecular weight of the GP sample was determined using a GE AKTA purifier 10 FPLC system equipped with a Superdex 200 10/300 GL column. Four polymers namely, bovine serum albumin (66.6 kDA), carbonic anhydrase (29.2 kDA), trypsin (23.3 kDA) and lysozyme (14.3 kDA) were used as standards prior to testing the GP sample. Zeta potential (ZP) of GP at different pH was measured using a dynamic light scattering technique on a nanoparticle analyzer SZ-100, Horiba Scientific. The ^{1}H NMR spectra of the GP sample was recorded using an NMR Spectrometer (AVANCE III-400 MHz, Bruker, Germany). The sample for NMR analysis was prepared by adding 10 mg of freeze-dried sample in 1 ml D_2O followed by heating at 60°C and sonication (30 min) for the complete dissolution of the sample.

3.5. Image acquisition and processing

Aggregates formed during the coagulation/flocculation process displayed fractal properties. After coagulation/flocculation, the formed flocs were prudently collected and transferred on to a flat microscope slide. Floc images were captured using an optical microscope fitted with a charge-coupled device (CCD) camera (Nikon Digital Sight–Fi1-U2) and analyzed further using an image processing software (Image J and Matrox Inspector 2.0). The images were acquired from an interrogation window of 1,280 × 960 with a resolution of 4.74 μm/ pixels. Fig. 2 depicts the schematic illustration of the experimental setup used for image analysis of flocs. Origin Pro 9.0 software was used for data analysis and graphing.

3.6. Fractal geometry

Fractal geometry concepts were used to describe the rugged surface of large, irregular, porous aggregates. Unlike in Euclidean geometry, objects packed heterogeneously with irregular boundaries were defined by nonlinear relationships by raising the properties such as area or volume of the object scale with a characteristic length dimension to the fractal dimension. The two-dimensional fractal dimension (D_2) of the flocs was calculated using a power-law relation between projected area (A) and the characteristic length (l) as

$$A \sim l^{D_2} \tag{3}$$

Large, highly branched and loosely bound aggregates have lower fractal dimensions whereas high fractal dimension results from densely packed aggregates ([Inline Equation] [4]. The D_2 value was calculated by regression analysis of the logarithm of A (projected area) vs. the logarithm of the characteristic length as indicated in Eq. (3) [14]. Perimeters (P) and projection areas (A) of flocs were calculated through

Fig. 2. Illustration of the experimental setup used for image analysis of flocs.

image analysis. The perimeter of the floc was taken as the characteristic length (l). The D_2 value was obtained from the slope of the line fitted to the data when area (A) was plotted on a log-log scale against perimeter (P) [see supplementary information (Figs. S1–S4) for detail].

3.7. Floc breakage and recovery

The floc strengths obtained under different conditions were compared in terms of strength factor (S_F). The higher the S_F value, the stronger the floc strength is. The S_F was determined by exposing the flocs to rapid mixing at 160 rpm for 1 min, followed by slow mixing (floc growth phase) at 40 rpm for 10 min. This was again followed by a rapid mixing at 160 rpm for 3 min (breakage phase), and subsequent slow mixing at 40 rpm for an additional 10 min. Theoretical floc strength was calculated by Eq. (2). The floc size was taken as the diameter of a circle of equivalent-area of floc image.

4. Results and discussion

4.1. Characterization of Grewia spp. biopolymer

4.1.1. Elemental analysis

Elemental analysis revealed that carbon, hydrogen (33.95% ± 0.07% and 6.07 %± 0.22%, respectively) are the major elements present in GP. The nitrogen content of the biopolymer was quite low (0.12% ± 0.03%). The results were very similar to the elemental composition of the banana stem (pseudostem) (C: 38.03%, H: 5.46%, and N: 0.42%) reported earlier by Alwi et al. [21]. A carbon to hydrogen ratio of 5.59 indicates the presence of carbon ring sugar monomeric units in the GP [21,22].

4.1.2. FTIR and ^{1}H NMR

FTIR spectra (Fig. 3) of the purified bio-flocculant revealed the presence of typical bands and peak characteristics of polysaccharides [23]. The band at 3,369 cm^{-1} indicated the presence of hydroxyl (–OH) group that might be due to the presence of atmospheric moisture or hydroxyl moieties of sugar rings. The band at 1,406 cm^{-1} could be due to the symmetric vibration of the –COOH group of glucuronic acid. The peaks at 1,675 and 1,558 cm^{-1} possibly indicated the
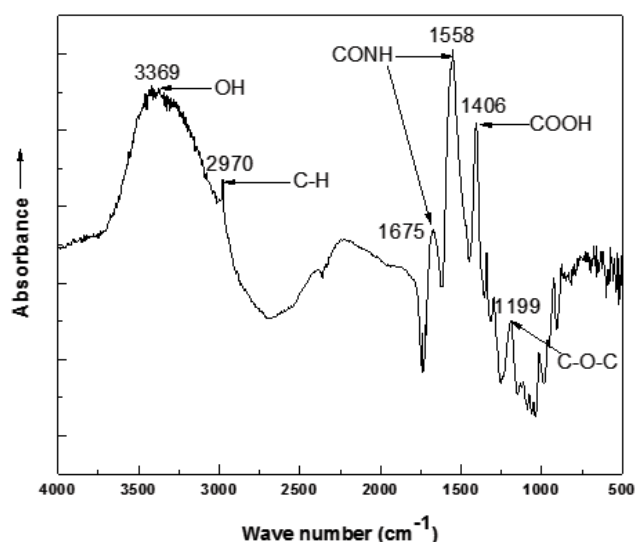
Fig. 3. FTIR spectrum of *Grewia* spp. biopolymer.

presence of –CONH group [24]. A number of peaks in the finger print region of the IR spectrum (800–1,200 cm^{-1}) could be accredited to the carbohydrates.

The ^{1}H NMR spectra of GP is shown in Fig. 4. The crowded spectrum in between 3 to 5 ppm is a typical representation of polysaccharide and evidence of similar sugar residues [23]. The signals at 1.06–1.15 and 1.84 may be attributed to the CH–CH$_3$ and COOCH$_3$ groups, respectively. The signals between 3.5–3.8 ppm belonged to the non-anomeric protons (H$_2$–H$_6$). Similarly, the broad signal between 4.3 to 5 ppm may be assigned to the beta-anomeric and alpha-anomeric protons [23,25]. Signals around 3.16 ppm could be accredited to the (–O–CH$_3$) group. The presence of the –CH$_3$ group suggested the presence of methylated sugar (rhamnose) in *Grewia* spp. biopolymer.

4.1.3. Zeta potential

The zeta potentials (ZP) of aqueous GP sample at pH 5, 7 and 9 were measured to be –18.96 ± 0.66 mV, –24.64 ± 0.49 and –30.45 ± 0.48, respectively. The results suggested the anionic nature of GP, and this could be ascribed to the presence of
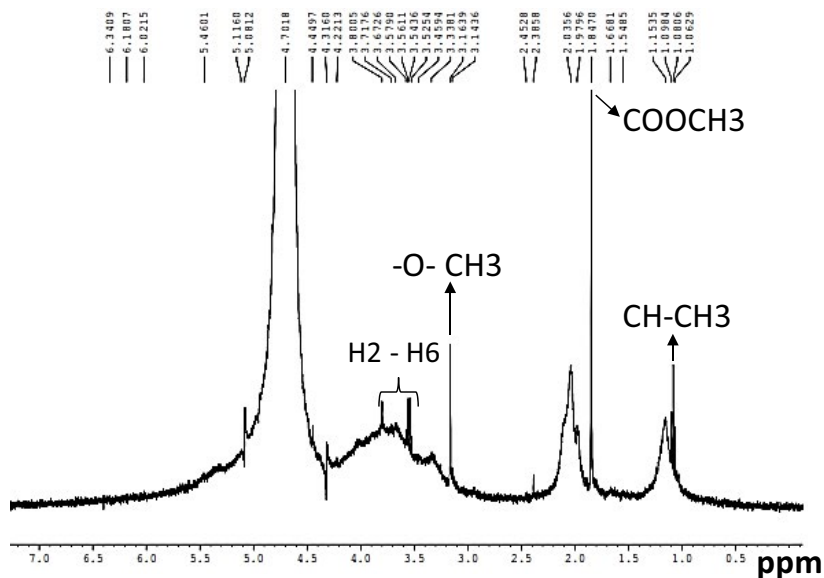
Fig. 4. ^{1}H NMR spectrum of *Grewia* spp. Biopolymer.

glucuronic acid, as confirmed by the FTIR spectrum (Fig. 3), in the polymer. This behavior of GP is in agreement with the previously reported findings [26,27].

4.1.4. Molecular weight

The molecular weight of GP was determined by gel permeation chromatography. The elution profiles revealed bimodal molecular weight (93,598.74 DA and 28,726.98 DA) distribution corresponding to the retention time of 15.31 and 37.57 min, respectively. Variation in molecular weight distribution of a polysaccharide depends on a number of factors including synthesis pathway, environment, and conditions used to isolate the materials [25]. In our case, the results were not in agreement with the earlier works [23,28]. This is presumably due to the difference in methodology or protocols followed for extraction and purification of the bio-polymer.

4.2. Image analysis and size distribution of flocs

Removal of turbidity or suspended particulates is the prime objective of coagulation-flocculation. Size, density and fractal dimension of flocs formed greatly influence the floc removal efficiency in this solid/liquid separation process. Smaller flocs contribute to residual turbidity. Thus, the number average size of flocs was determined from image analysis. The optical micrographs and the corresponding size distribution profiles of the flocs formed using a different coagulant and in combination with GP at pH 7 are shown in Fig. 5. Derived number of average flocs sizes are also mentioned in Fig. 5. Floc formation, re-growth after breakage were investigated to understand and reversibility of breakage of flocs formed using different coagulation mechanisms. Characteristics of flocs exposed to high shear are dictated by the floc strength and ability of the broken flocs to re-grow. Reversibility of floc breakage, that is, regrowth of the broken flocs to their original size before breakage, indicates that the sludge can be reused to decrease the coagulant demand. As evident from Figs. 5a, b, e, and f the number average floc sizes before and after breakage were in close proximity indicating that broken laterite flocs partially re-grew when iron sulfate or alum were used as a coagulant. Also, the flocs sizes with number average floc sizes varying between ~105 to 150 μm were not very large.

The addition of GP along with inorganic coagulants (alum- or iron-based) resulted in the formation of larger aggregates (number average floc sizes ~ 1,000–1,500 μm) as compared to loosely bound floc structures obtained using only inorganic coagulant. Moreover, in the presence of a GP biopolymer, the broken flocs could re-grow to a much greater extent indicating almost fully reversible flocs breakage (Figs. 5c, d, g, and h). The differences in floc sizes and degree of reversibility in floc breakage in the absence or presence of a GP biopolymer may be due to different coagulation mechanisms [29]. In general, at an optimal dosage of inorganic coagulants sweep coagulation is the main mechanism resulting in the formation of larger flocs. In such cases, complete re-growth of broken flocs to their initial size before the breakage is quite difficult. However, in the case of laterite suspension, inorganic coagulant-induced coagulation led to the formation of smaller flocs that showed significant floc breakage reversibility. Therefore, it may be deduced that charge neutralization is the dominant mechanism in the coagulation of laterite suspension using inorganic coagulant.

Zeta potential measurement revealed that GP biopolymer is anionic in nature. Therefore, the formation of larger flocs in the presence of a GP biopolymer indicates flocculation of alum or iron-coagulated laterite particles primarily through charge neutralization. This is complemented by the entrapment of solid particles through bridging flocculation due to high molecular weight, long-chain biopolymer [30–32]. The flocs formed due to bridging flocculation are much stronger than those produced when particles are coagulated using simple inorganic salts. Flocs produced using polymeric
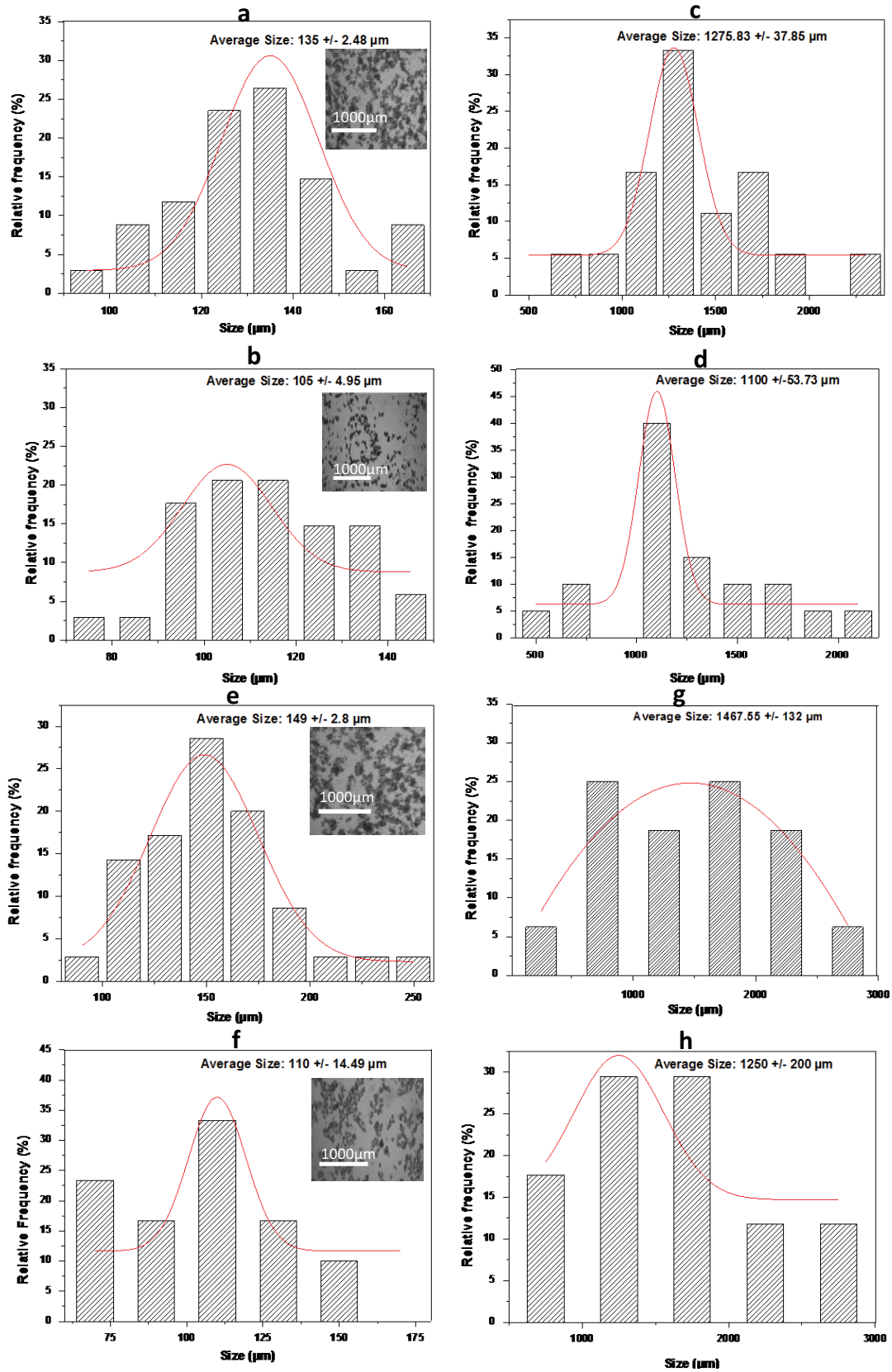
Fig. 5. Size distribution profiles and optical micrographs (insets) of flocs formed by alum, iron sulfate and *Grewia* spp. biopolymer (GP) flocculation at pH 7: (a) iron flocs, (b) iron flocs after breakage, (c) iron flocs with GP, (d) iron flocs with GP after breakage, (e) alum flocs, (f) alum flocs after breakage, (g) alum flocs with GP, and (h) alum flocs with GP after breakage.

Table 1
Effect of *Grewia* spp. biopolymer on fractal dimension and floc strength at different pH

Experimental conditions	Fractal dimension	$R^{2\#}$	Strength factor (%)
Iron floc (pH 9)	1.23 ± 0.04	0.98	51.22
Iron floc (pH 9) post-floc breakage	1.17 ± 0.06	0.92	
Iron floc (pH 9) + GP	1.62 ± 0.09	0.98	81.58
Iron floc (pH 9) + GP post-floc breakage	1.53 ± 0.06	0.96	
Alum floc (pH 9)	1.23 ± 0.07	0.98	56.38
Alum floc (pH 9) post-floc breakage	1.13 ± 0.04	0.98	
Alum floc (pH 9) + GP	1.62 ± 0.11	0.98	91.80
Alum floc (pH 9) + GP post-floc breakage	1.57 ± 0.16	0.98	
Iron floc (pH 7)	1.29 ± 0.06	0.97	55.70
Iron floc (pH 7) post-floc breakage	1.26 ± 0.05	0.95	
Iron floc (pH 7) + GP	1.75 ± 0.14	0.99	94.99
Iron floc (pH 7) + GP post-floc breakage	1.55 ± 0.11	0.94	
Alum floc (pH 7)	1.28 ± 0.07	0.96	54.81
Alum floc (pH 7) post-floc breakage	1.20 ± 0.07	0.94	
Alum floc (pH 7) + GP	1.64 ± 0.08	0.99	87.30
Alum floc (pH 7) + GP post-floc breakage	1.52 ± 0.09	0.99	
Iron floc (pH 5)	1.27 ± 0.09	0.97	59.94
Iron floc (pH 5) post-floc breakage	1.24 ± 0.08	0.95	
Iron floc (pH 5) + GP	1.84 ± 0.12	0.99	92.41
Iron floc (pH 5) + GP post-floc breakage	1.67 ± 0.33	0.97	
Alum floc (pH 5)	1.24 ± 0.06	0.93	55.48
Alum floc (pH 5) post-floc breakage	1.24 ± 0.08	0.95	
Alum floc (pH 5) + GP	1.75 ± 0.07	0.95	91.50
Alum floc (pH 5) + GP post-floc breakage	1.57 ± 0.14	0.99	

#R^2 is the regression coefficient between floc projected area and floc perimeter plotted in a Log-Log scale

flocculants are, therefore, significantly more resistant to breakage [30].

4.3. Fractal dimension and strength factor

The two-dimensional fractal dimensions and strength factor of flocs formed under different conditions are presented in Table 1.

The flocs formed in the presence of GP were more compact and had higher fractal dimensions compared to those produced by coagulants alone. Flocs were more compact in lower pH. An increase in pH led to the formation of a looser floc structure (Figs. 6I and II). Fractal dimensions of only iron-coagulated flocs (1.27 ± 0.09, 1.29 ± 0.06 and 1.23 ± 0.04 at pH 5, 7, and 9, respectively) increased in presence of GP (1.84 ± 0.12, 1.75 ± 0.14 and 1.62 ± 0.09). Floc strength (51.22%–59.94%) also got increased to 81.58%–94.99%. Similarly alum-coagulated flocs (floc strength: 54.81%–56.38% and fractal dimensions 1.24 ± 0.06, 1.28 ± 0.07 and 1.23 ± 0.07 at pH 5, 7 and 9, respectively) became more compact in presence of the biopolymer (floc strength 87.30%–91.80% and fractal dimensions 1.75 ± 0.07, 1.64 ± 0.08, 1.62 ± 0.11 at pH 5, 7 and 9, respectively). The results were in excellent agreement with the findings of image analysis (Fig. 5). The fractal dimension values of alum- or iron- coagulated flocs were very close to each other. However, iron flocs had a slightly higher fractal dimension than alum flocs indicating that iron flocs had a more compact structure [33].

At higher pH (above neutral), the flocs were made predominantly by adsorption and sweep flocculation, where the physical links play an important role within flocs rather than the chemical bond that commonly occurred at lower pH [34]. At lower pH, when active species of the coagulants are positively charged, the synergetic action between coagulants and GP resulted in the formation of flocs with higher fractal dimension by both charge neutralization and bridging mechanism.

The floc strength factor depends on coagulant and pH. When alum or alum and GP were used, floc strength did not change much over the studied pH range (5–9) except a little dip around neutral pH (Fig. 6III). However, when iron was used as a coagulant floc strength decreased significantly above neutral pH (pH 9). This may be explained by the variation of zeta potential and inner chemical bonds [35]. It has already been shown that flocs made by charge neutralization (lower pH) attain higher strength. In our case, at lower pH when inorganic coagulant was dosed hydrolyzed Al or Fe species were predominantly positively charged and charge neutralization was the primary mechanism. At elevated pH (near neutral above) sufficient amorphous metal
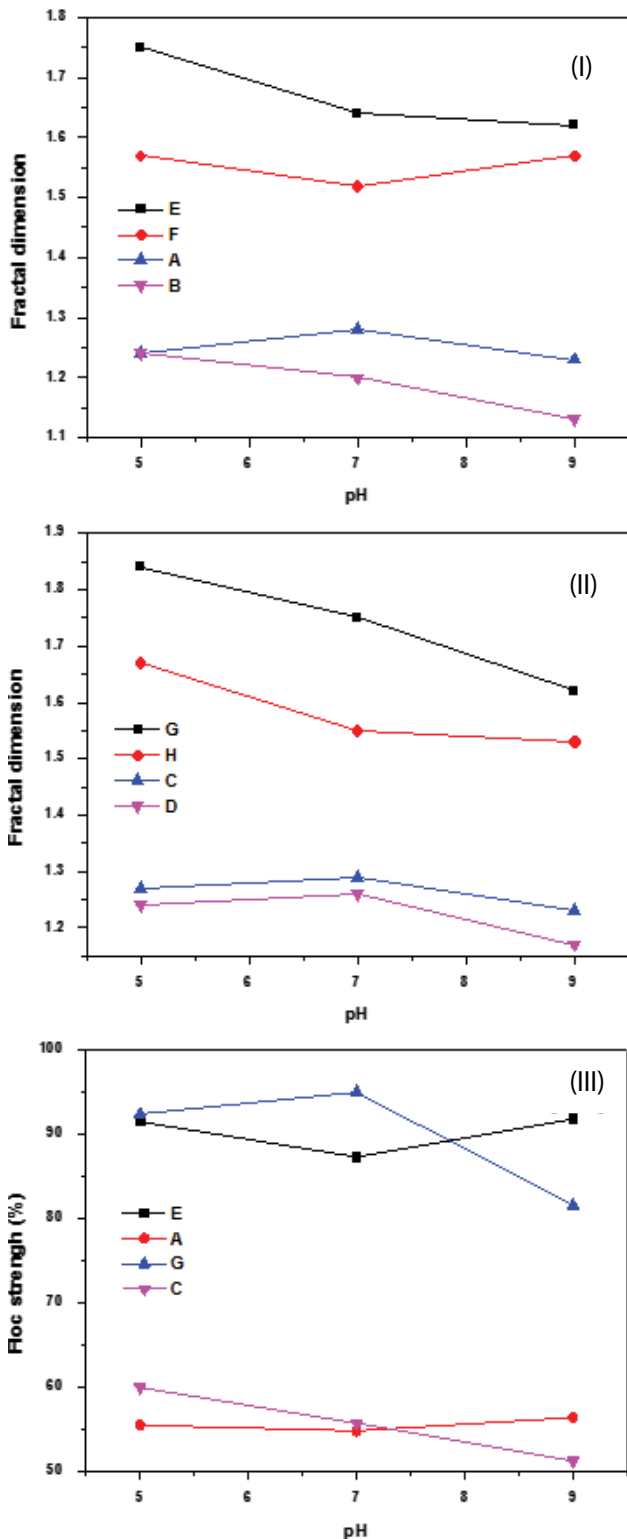
Fig. 6. Effect of *Grewia* spp. biopolymer on fractal dimension (I & II) and floc strength (III) at different pH after formation and re-growth; (A) alum flocs, (B) alum flocs after breakage, (C) iron flocs, (D) iron flocs after breakage, (E) alum flocs + GP, (F) alum flocs + GP after breakage, (G) iron flocs + GP, and (H) iron flocs + GP after breakage.

hydroxide species were formed leading to sweeping flocculation. Flocs formed following charge neutralization mechanisms usually have higher strength.

Flocs formed in presence of GP had higher floc strength. Higher molecular weight polymers should lead to formation of stronger aggregates though polymer bridging or 'electrostatic patch' effects [3]. Addition of GP favored adsorption bridging effect and thus, augmented the floc strength resisting floc fragmentation to the minimal.

5. Conclusion

Effects of addition of *Grewia* spp. biopolymer on the floc properties of laterite flocs formed by using two common coagulants, aluminum sulfate and ferric sulfate were investigated. Biopolymer produced from *Grewia* spp. barks were characterized as a high molecular weight polymer of anionic nature. Polysaccharides in the biopolymer were recognized as the major active constituent responsible for its flocculating property. Fractal dimension, structure, and strength of flocs were monitored by a non-invasive image analysis tool. Fractal dimension and strength of flocs formed in presence of GP were higher than those of flocs formed by using inorganic coagulants only. The addition of GP resulted in more compact floc that showed significant reversibility of floc breakage. The broken flocs returned to their initial size before breakage when *Grewia* spp. the biopolymer was used as a coagulant aid.

Symbols

M	—	Coagulated mass
R	—	Size of coagulated mass
D_F	—	Mass fractal dimension
S_F	—	Floc strength factor
d_1	—	Diameter of a formed floc
d_2	—	Diameter of a broken floc
A	—	Projected area of floc
l	—	Characteristic length of floc
P	—	Perimeter of floc
D_2	—	Two-dimensional fractal dimension

References

[1] P. Jarvis, B. Jefferson, S.A. Parsons, Breakage, re-growth, and fractal nature of natural organic matter flocs, Environ. Sci. Technol., 39 (2005) 2307–2314.

[2] C.Y. Teh, P.M. Budiman, K.P.Y. Shak, T.Y. Wu, Recent advancement of coagulation-flocculation and its application in wastewater treatment, Ind. Eng. Chem. Res., 55 (2016) 4363–4389.

[3] M.A. Yukselen, J. Gregory, The reversibility of flocs breakage, Int. J. Miner. Process., 73 (2004) 251–259.

[4] J. Gregory, The density of particle aggregates, Water Sci. Technol., 36 (1997) 1–13.

[5] Y. Zhao, Correlations between floc physical properties and optimum polymer dosage in alum sludge conditioning and dewatering, Chem. Eng. J., 92 (2003) 227–235.

[6] Y. Sang, P. Englezos, Flocculation of precipitated calcium carbonate (PCC) by cationic tapioca starch with different charge densities. I: Experimental, Colloids Surf., A., 414 (2012) 512–519.

[7] M.A. Yukselen, J. Gregory, The effect of rapid mixing on the break-up and reformation of flocs, J. Chem. Technol. Biotechnol., 79 (2004) 782–788.

[8] J. Gregory, Monitoring floc formation and breakage, Water Sci. Technol., 50 (2004) 163–170.

[9] T. Li, Z. Zhu, D.S. Wang, C.H. Yao, H.X. Tang, The strength and fractal dimension characteristics of alum–kaolin flocs, Int. J. Miner. Process., 82 (2007) 23–29.

[10] I. Solomentseva, S. Barany, J. Gregory, The effect of mixing on stability and break-up of aggregates formed from aluminum sulfate hydrolysis products, Colloids Surf., A, 298 (2007) 34–41.

[11] K.P.Y. Shak, T.Y. Wu, Synthesis and characterization of a plant-based seed gum via etherification for effective treatment of high-strength agro-industrial wastewater, Chem. Eng. J., 307 (2017) 928–938.

[12] W.W. Li, W.Z. Zhou, Y.Z. Zhang, J. Wang, X.B. Zhu, Flocculation behavior and mechanism of an exopolysaccharide from the deep-sea psychrophilic bacterium *Pseudoalteromonas* sp. SM9913, Bioresour. Technol., 99 (2008) 6893–6899.

[13] M.F. Elkady, S. Farag, S. Zaki, G. Abu-Elreesh, D. Abd-El-Haleem, *Bacillus mojavensis* strain 32A, a bioflocculant-producing bacterium isolated from an Egyptian salt production pond, Bioresour. Technol., 102 (2011) 8143–8151.

[14] G.C. Bushell, Y.D. Yan, D. Woodfield, J. Raper, R. Amal, On techniques for the measurement of the mass fractal dimension of aggregates, Adv. Colloid Interface Sci., 95 (2002) 1–50.

[15] R.M. Wu, D.J. Lee, T.D. Waite, J. Guan, Multilevel structure of sludge flocs, J. Colloid Interface Sci., 252 (2002) 383–392.

[16] R.K. Chakraborti, J.F. Atkinson, J.E.V. Benschoten, Characterization of alum floc by image analysis, Environ. Sci. Technol., 34 (2000) 3969–3976.

[17] J. Gregory, Monitoring particle aggregation processes, Adv. Colloid Interface Sci., 147–148 (2009) 109–123.

[18] S. Byun, J. Oh, B.Y. Lee, S. Lee, Improvement of coagulation efficiency using instantaneous flash mixer (IFM) for water treatment, Colloids Surf., A, 268 (2005) 104–110.

[19] J.F. Yu, D.S. Wang, M.Q. Yan, C.Q. Ye, M. Yang, X.P. Ge, Optimized coagulation of high alkalinity, low temperature and particle water: pH adjustment and polyelectrolytes as coagulant aids, Environ. Monit. Assess., 131 (2007) 377–386.

[20] P. Somboonpanyakul, Q. Wang, W. Cui, S. Barbut, P. Jantawat, Malva nut gum. (Part I): extraction and physicochemical characterization, Carbohydr. Polym., 64 (2006) 247–253.

[21] H. Alwi, J. Idris, M. Musa, K.H.K. Hamid, A preliminary study of banana stem juice as a plant-based coagulant for treatment of spent coolant wastewater, J. Chem., 2013 (2013) 1–7.

[22] V.T.P. Vinod, R.B. Sashidhar, K.I. Suresh, B.R. Rao, U.V.R.V. Saradhi, T.P. Rao, Morphological, physico-chemical and structural characterization of gum kondagogu (*Cochlospermum gossypium*): a tree gum from India, Food Hydrocolloids, 22 (2008) 899–915.

[23] E.I. Nep, R.C. Barbara, Characterization of *Grewia* gum, a potential pharmaceutical excipient, J. Excipients Food Chem., 1 (2010) 30–40.

[24] M.P. Filippov, Practical infrared spectroscopy of pectic substances, Food Hydrocolloids, 6 (1992) 115–142.

[25] S.W. Cui, Structural Analysis of Polysaccharides, S.W. Cui, ed., Food Carbohydrates: Chemistry, Physical Properties, and Applications, Taylor and Francis Group, Boca Raton, 2005, pp. 105–157.

[26] N. Georgiadis, C. Ritzoulis, G. Sioura, P. Kornezou, C. Vasiliadou, and C. Tsioptsias, Contribution of okra extracts to the stability and rheology of oil-in-water emulsions, Food Hydrocolloids, 25 (2011) 991–999.

[27] M.A. Mohammadifar, S.M. Musavi, A. Kiumarsi, P.A. Williams, Solution properties of targacanthin (water-soluble part of gum tragacanth exudates from *Astragalus gossypinus*), Int. J. Biol. Macromol., 38 (2006) 31–39.

[28] J.O. Ikoni, S.O. Ignatius and W.H. Stephen, *Grewia* gum as a potential aqueous film coating agent. I: Some physicochemical characteristics of fractions of *Grewia* gum, J. Pharm. BioAllied Sci., 5 (2013) 53–60.

[29] Y. Wenzheng, J. Gregory, L.C. Campos, Breakage and re-growth of flocs formed by charge neutralization using alum and polyDADMAC, Water Res., 44 (2010) 3959–3965.

[30] N. Meiqing, W. Zhang, D. Wang, Y. Chen, R. Chen, Correlation of physicochemical properties and sludge dewaterability under chemical conditioning using inorganic coagulants, Bioresour. Technol., 144 (2013) 337–343.

[31] T. Li, Z. Zhu, D. Wang, C. Yao, H. Tang, Characterization of floc size, strength and structure under various coagulation mechanisms, Powder Technol., 168 (2006) 104–110.

[32] Z. Yang, H.J. Li, H. Yan, H. Wu, H. Yang, Evaluation of a novel chitosan based flocculant with high flocculation performance, low toxicity and good floc properties, J. Hazard. Mater., 276 (2014) 480–488.

[33] C. Turchiuli, C. Fargues, Influence of structural properties of alum and ferric flocs on sludge dewaterability, Chem. Eng. J., 103 (2004) 123–131.

[34] X. Weiying, G. Baoyu, Y. Qinyan, B. Xiaowen, Influence of pH on flocs formation, breakage and fractal properties — the role of Al 13 polymer, J. Water Sustainability, 1 (2011) 45–57.

[35] R. Li, B. Gao, X. Huang, H. Dong, X. Li, Q. Yue, Y. Wang, Q. Li, Compound bioflocculant and polyaluminum chloride in kaolin-humic acid coagulation: factors influencing coagulation performance and floc characteristics, Bioresour. Technol., 172 (2014) 8–15.

Supplementary information
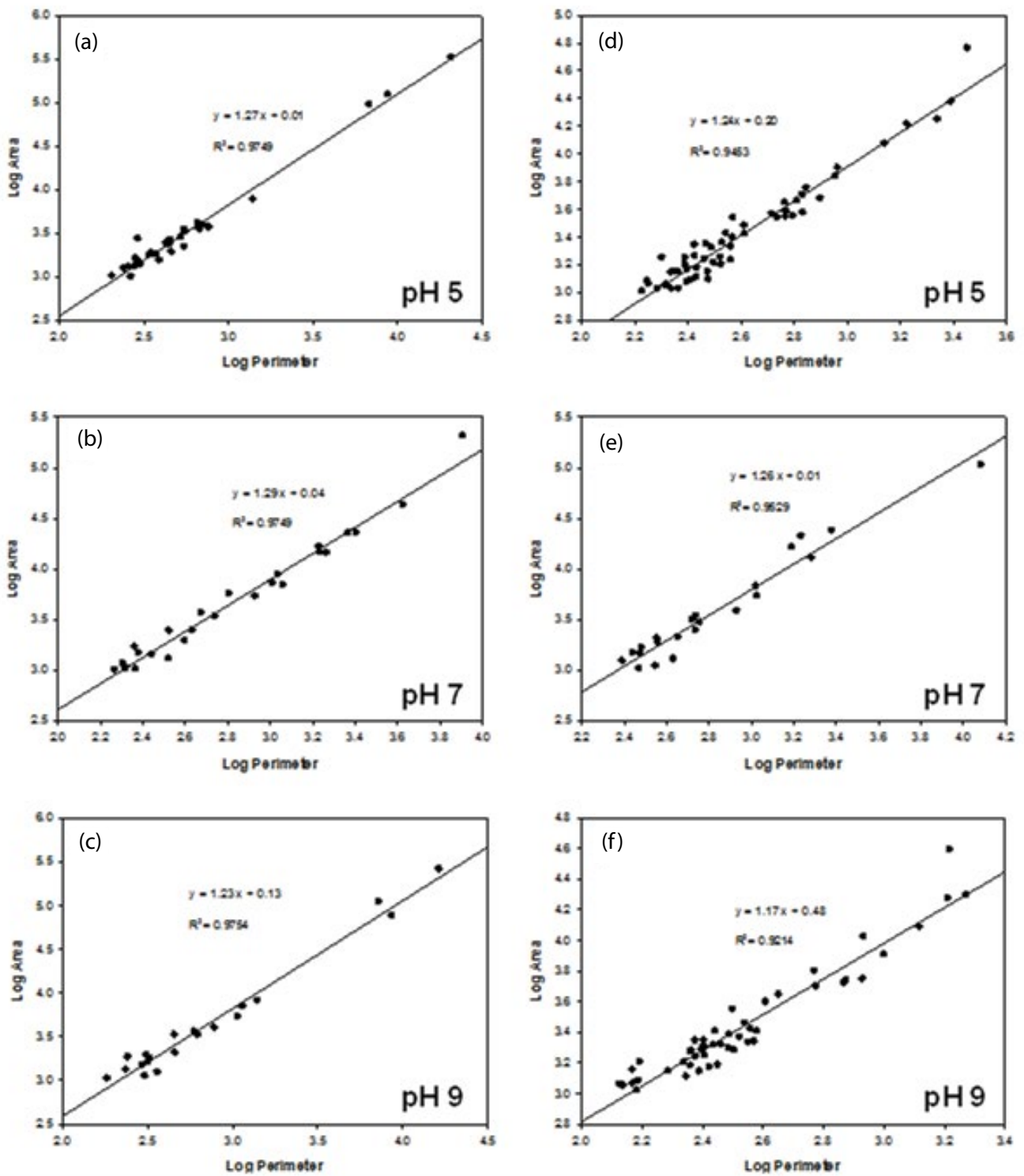
Fig. S1. Plot of the projected area and perimeter of iron-coagulated laterite flocs at different pH; after formation (a–c) and breakage (d–f).
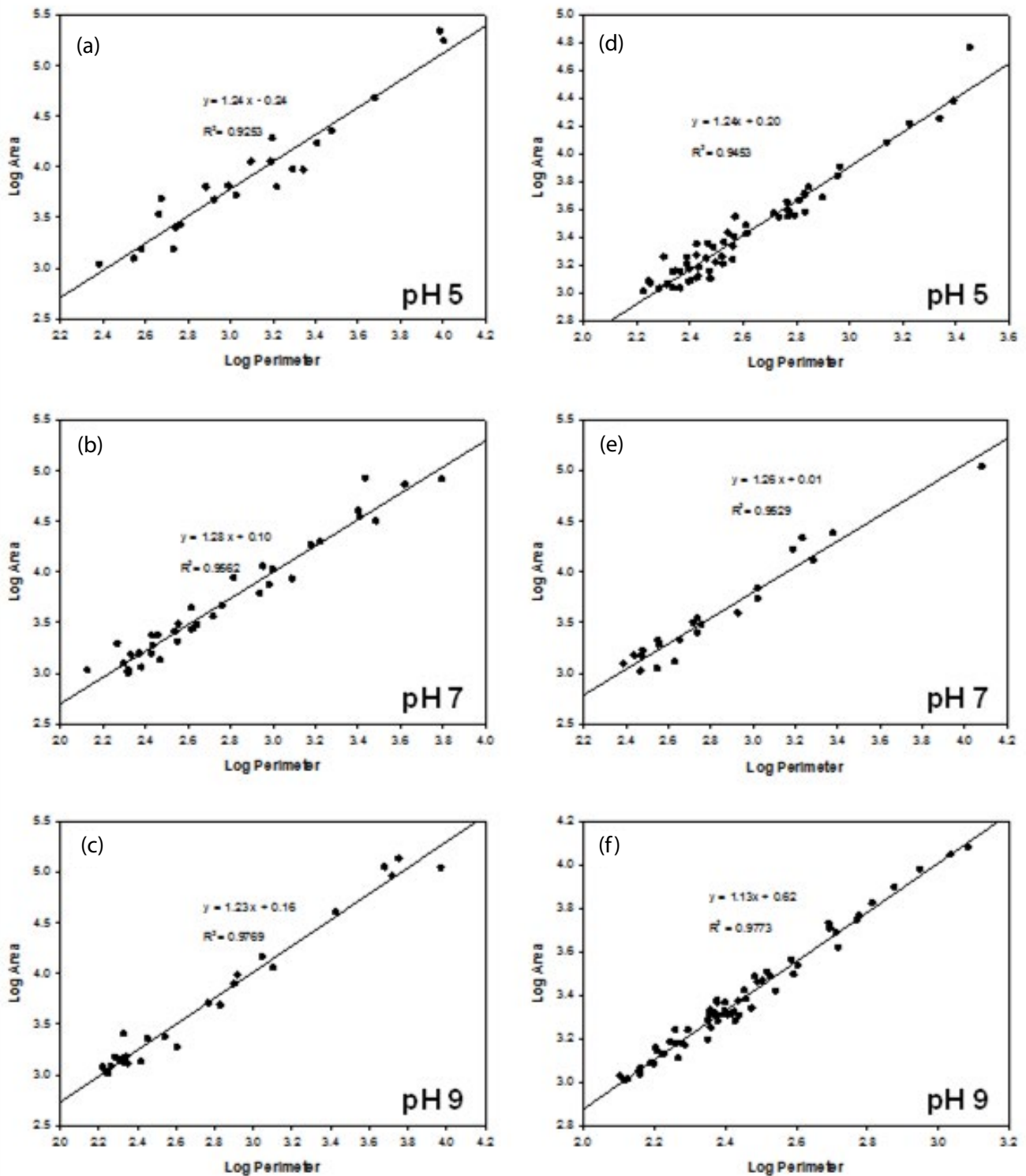
Fig. S2. Plot of the projected area and perimeter of alum-coagulated laterite flocs at different pH; after formation (a–c) and breakage (d–f).
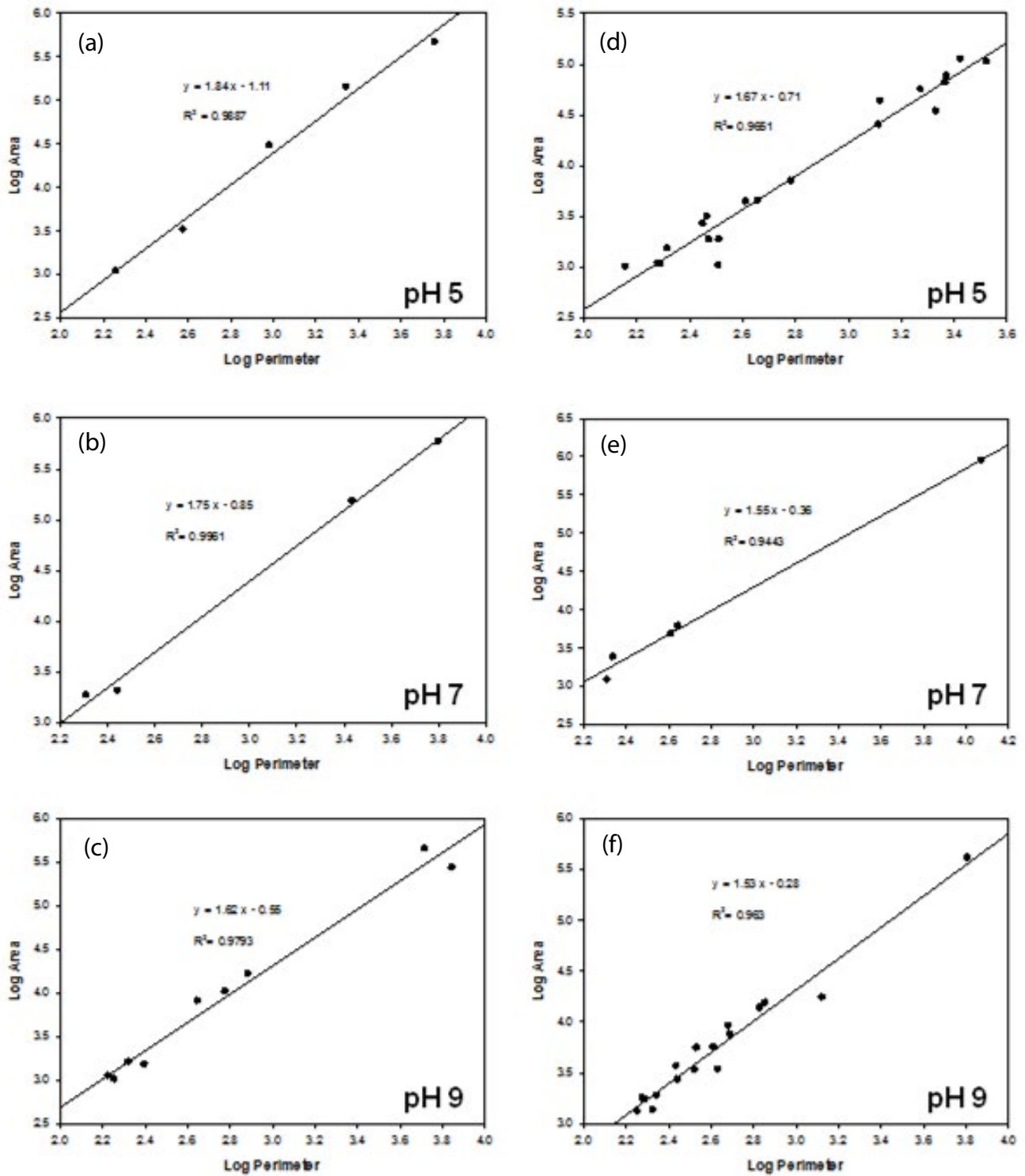
Fig. S3. Plot of the projected area and perimeter of (iron + *Grewia* biopolymer)-coagulated laterite flocs at different pH; after formation (a–c) and breakage (d–f).
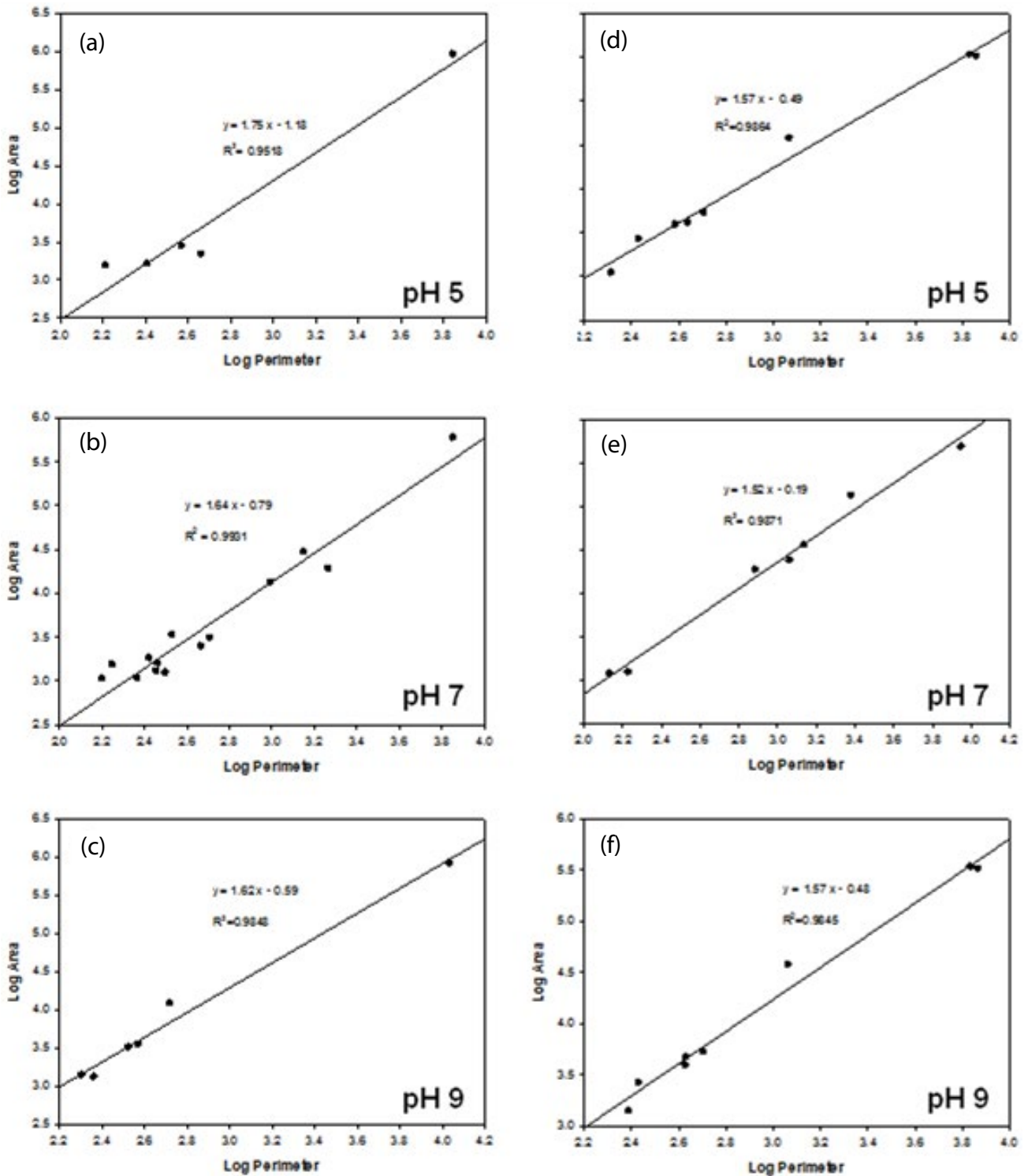
Fig. S4. Plot of the projected area and perimeter of (alum + *Grewia* biopolymer)-coagulated laterite flocs at different pH; after formation (a–c) and breakage (d–f).